

# Tunneling hot-electron transfer amplifier: A hot-electron GaAs device with current gain

M. Heiblum, D. C. Thomas, C. M. Knoedler, and M. I. Nathan  
IBM Thomas J. Watson Research Center, Yorktown Heights, New York 10598

(Received 22 July 1985; accepted for publication 29 August 1985)

Tunneling hot-electron transfer amplifier (THETA) devices, based on GaAs-AlGaAs heterojunctions, were fabricated and tested. Hot-electron transfer ( $\alpha$ ) through a 1100-Å base in excess of 70% was found at 4.2 K. This resulted in a corresponding current gain ( $\beta$ ) in a common emitter configuration of about 2.3. In the temperature range of 4.2–80 K and under constant biasing conditions,  $\alpha$  was nearly temperature independent. Electron energy distributions for motion normal to the layers and electron total energy loss while traversing the device were estimated. Typical widths of the energy distributions were less than 200 meV, and both widths and energy peak positions were only slightly dependent on temperature and initial injection energy.

The first proposal of a tunneling hot-electron transfer amplifier (THETA) device was published in 1960 by Mead, who named it cold cathode transistor (CCT).<sup>1</sup> Electrons were injected through a very thin oxide barrier (15–25 Å wide) into a thin metal “base” (about 100 Å wide) and collected above another thin barrier. The device, in principle, was very fast but difficult to realize experimentally. In 1981 Heiblum proposed the heterojunction THETA device.<sup>2</sup> This device is analogous to the CCT device, but the metals were replaced by  $n^+$ -GaAs and the oxides by undoped AlGaAs. Recently, based on the same principles, barriers were made by modulating the energy bands in  $n$ -Si (by  $p$ -type implantation, forming the Camel transistor),<sup>3</sup> and in  $n$ -GaAs [utilizing planar  $p$ -type doping by molecular beam epitaxy (MBE), forming the planar doped barrier transistor (PDBT)].<sup>4–6</sup> The first realization of the heterojunction THETA device was reported recently by Yokoyama *et al.*,<sup>7</sup> who measured a transfer coefficient of 0.57 at 40 K. We report here a relatively simple fabrication process for a heterojunction THETA device which exhibits a transfer coefficient of 70% and a corresponding current gain exceeding 2 at 4.2 K. This device was also utilized to study energy distributions of the hot electrons.

Figure 1 describes the energy-band diagram of our THETA device under normal biasing conditions in a common base configuration. The applied voltage  $V_{BE}$  causes electrons to tunnel from emitter to base, through the 110 Å of the undoped Al<sub>0.35</sub>Ga<sub>0.65</sub>As, resulting in an emitter current  $I_E$ . The tunneling electrons enter the base with an excess kinetic energy, which approaches approximately  $eV_{BE}$  at the end of the depletion layer in the base (if scattering is neglected). If this energy is larger than the effective collector barrier height  $\Phi'_c$ , which is formed by the graded undoped Al<sub>0.25</sub>Ga<sub>0.75</sub>As, some of the hot electrons will surmount this barrier and produce a collector current  $I_C$ , with a transfer coefficient  $\alpha \equiv I_C/I_E$ . In a common emitter configuration a current gain is defined as  $\beta \equiv I_C/I_B$ , where  $I_B$  is the base current.

The device structure was grown in an MBE system on a (100) oriented  $n^+$ -GaAs substrate, which was previously heat treated and polished. After a routine cleaning procedure<sup>8</sup> a 1- $\mu$ m-thick conductive GaAs buffer layer was

grown. It was Si doped to  $2 \times 10^{18}$  cm<sup>-3</sup> in the first 1500 Å near the substrate interface and to  $4 \times 10^{17}$  cm<sup>-3</sup> thereafter. This layer was followed by the collector barrier composed of Al<sub>0.25</sub>Ga<sub>0.75</sub>As, (undoped, 1000 Å total thickness), which was graded over 200 Å near the base to  $x = 0.12$  (by reducing the Al flux). The GaAs base ( $2 \times 10^{17}$  cm<sup>-3</sup>, 1100 Å), the Al<sub>0.35</sub>Ga<sub>0.65</sub>As emitter barrier (undoped, 110 Å), and the top GaAs emitter ( $2 \times 10^{17}$  cm<sup>-3</sup>, 2500 Å) were subsequently grown. In the fabrication process we used boron implantation for isolation, reactive ion etching and wet etching to form the emitter mesa, and alloyed AuGeNi for ohmic contacts. The ohmic contacts were done by evaporating Ni (50 Å)-Au (450 Å)-Ge (150 Å) and alloying them for about 5 s at 420 °C. The emitter contact dimensions were  $5 \times 20$   $\mu$ m<sup>2</sup>. The base contact was composed of two separate contacts on both sides of the emitter mesa and 5  $\mu$ m away from its boundaries. Processed devices were very uniform in their characteristics and exhibited a high yield.

When the device is operated at room temperature, thermally activated currents are dominant and overwhelm the tunneling currents. When the operating temperature is reduced, the thermal currents diminish and both emitter and collector barriers restrict current flow effectively. For example, base-emitter and base-collector barriers have distinct thresholds of 0.4 and 1 V, respectively, at 4.2 K. Figure 2 is a typical family of output curves measured in a common base configuration at 4.2 K, where  $I_E$  is the parameter. For  $I_E = 0$  the collector current  $I_C$  remains very small up to about 1 V; thereafter it rises rapidly. This can be due to Fowler–Nordheim tunneling through the distorted collector barrier, which has an effective estimated thickness of about 130 Å for the base Fermi electrons, or due to carrier spillover above the barrier top which is only some 20 meV high relatively to the Fermi electrons under these biasing conditions. When  $I_E = 20$   $\mu$ A, for example,  $I_C$  rises with  $V_{CB}$ , resulting in an average output differential resistance of  $\approx 80$  k $\Omega$ .  $I_C$  decreases to zero only for  $V_{CB} < 0$ , as expected from the band diagram shown in Fig. 1. For higher  $I_E$ , the output differential conductance is larger, but  $\alpha$  remains constant up to about 1 mA and depends only on  $V_{CB}$ . The device operates with currents as high as 5 mA without any irreversible degradation in its characteristics.

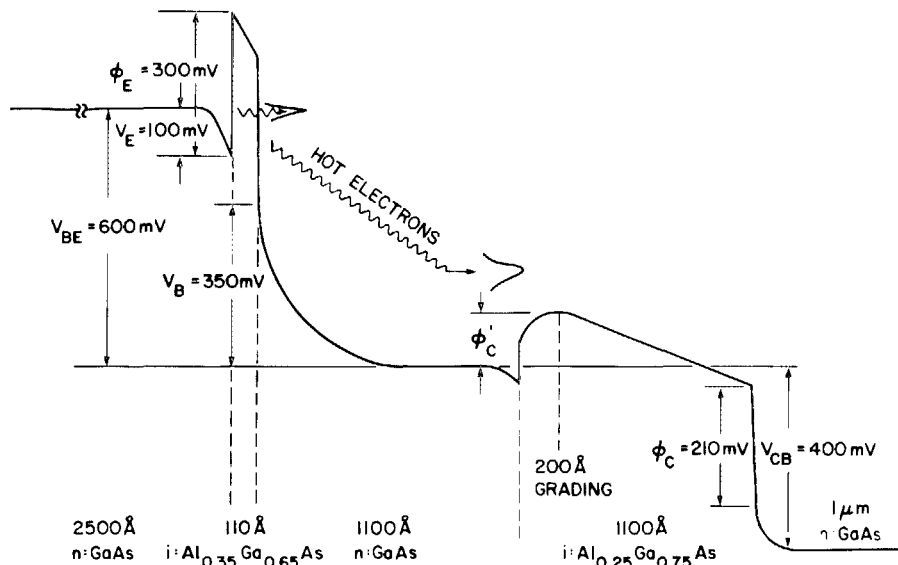


FIG. 1. Description of the energy diagram of the heterojunction THETA device. Estimated potential distribution for  $\Gamma$  electrons, and the specific device parameters are noted. For the emitter tunneling barrier only a small fraction of  $V_{BE}$  is across the AlGaAs barrier. The Fermi level is not shown, but it is some 18 meV above the conduction band at 4 K. The accumulation layer in the base bends the conduction band by about 60 meV.

The base spreading resistance  $r_b$  is a common resistance for both emitter and collector circuits. Since  $r_e$  and  $r_c$  are small, the true biases are  $V'_{BE} = V_{BE} - I_B r_b$  and  $V'_{CB} = V_{CB} + I_B r_b$ . Using the split base contact we can measure a resistance  $r_{bb}$ , and estimate  $r_b$  to be about 500  $\Omega$ . From Fig. 2 one can deduce, conservatively, that  $\alpha_{max} = 0.7$  for  $V_{CB} = 900$  mV, a region where  $I_B r_b$  is not yet important. In the temperature range 4.2–80 K,  $\alpha$  is temperature independent for a constant bias. At higher temperature (up to 160 K) it decreases by some 30%.

The characteristics of the same device operating in a common emitter mode are shown in Fig. 3. The collector current rises only for  $V_{CE} > 0.7$  V, since only then is  $V_{CB} > 0$ . As shown in some more detail by the inset in the figure, at small currents and a fixed  $V_{CE}$ , with the increase of  $I_B$  and consequently  $V_{BE}$ ,  $I_C$  decreases due to the decrease of  $V_{CB}$ . At higher voltages, where  $I_C$  is only weakly dependent on  $V_{CB}$  but fulfills  $I_C = \beta I_B$ , the curves cross each other. For  $V_{CE} = 1.6$  V (which corresponds to  $V_{CB} \approx 0.9$  V), the maximum measured current gain is  $\beta \approx 2.3$  and is almost independent of  $I_E$ . This value corresponds well with the maximum value of  $\alpha$ .

The derivative  $G_C = dI_C/dV_{CB}$  for  $V_{CB} < 0$  gives the

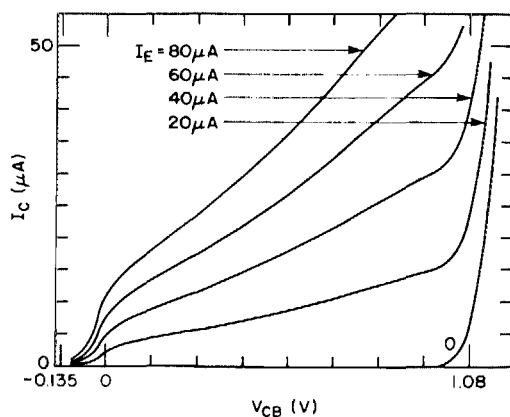


FIG. 2. Output characteristics of the THETA device operated at 4.2 K in a common base configuration, where  $I_E$  is the parameter. The transfer coefficient  $\alpha$ , output differential resistance, and electron normal energy distribution were deduced from these curves.

energy distribution of the electrons associated with their motion normal to the heterojunction planes. The peak is the most probable energy,  $E_p$ , of the collected hot electrons at the collector interface relative to the conduction-band minimum in the base. From Figs. 1 and 4,  $E_p = \Phi_C + |eV_{peak}|$ , where  $V_{peak}$  is the position of the peak in Fig. 4. Even though  $V_{peak}$  seems to increase with  $V_{BE}$ , corrections for the contribution of  $I_B r_b$  lead to a true  $V_{peak} \approx 0$  for all  $I_E$  or  $V_{BE}$ . As will be discussed later, the interpretation of the energy distributions is more involved because they are centered around  $V_{CB} = 0$ .

Estimating the potential distribution in the collector region is complicated by the graded AlGaAs region; thus Fig. 1 shows quantitatively only the calculated potential in the emitter and base regions. Barrier heights are assumed using  $\Delta E_C \approx 0.6 \Delta E_g$ .<sup>9-11</sup> By grading the collector barrier we have attempted to reduce the quantum mechanical reflections and achieve a bias-dependent barrier height ( $\Phi'_C$ ). Although this increases the collection efficiency, it also increases, unavoidably, the output differential conductance. Moreover, hot electrons that thermalize in the initial 200  $\text{\AA}$  of the AlGaAs will not be collected due to the retarding field, thus increasing the effective base thickness. The relatively low base doping ( $2 \times 10^{17} \text{ cm}^{-3}$ ) reduces impurities and plasmon

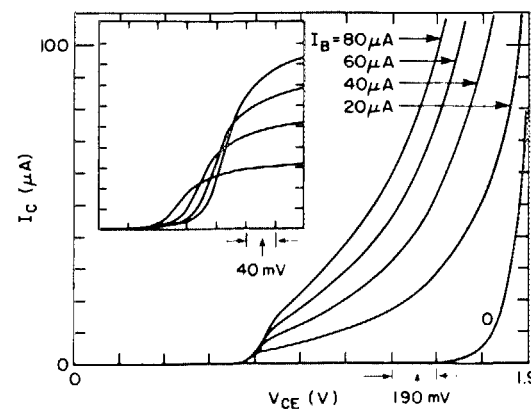


FIG. 3. Output characteristics of the device at 4.2 K, in a common emitter configuration, where  $I_B$  is the parameter. The inset shows an expansion of the region of the initial current onset.

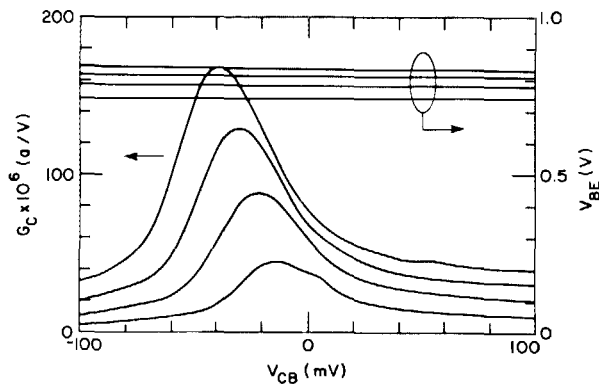


FIG. 4. Apparent energy distributions of the collected hot electrons, where  $I_E$  is the parameter. The actual energy of the electrons is  $\Phi_C + |V_{CB}| - I_B r_b$  for  $V_{CB} < 0$ .  $V_{BE}$  vs  $V_{CB}$  is also shown for each  $I_E$ . For the lowest curve  $I_E = 0$ , and it increases by 20- $\mu$ A steps.

scattering,<sup>5</sup> but causes a relatively high base spreading resistance.

Assuming an exponential decay of  $\alpha$  with increasing base width, we find an effective mean free path  $\lambda \simeq 2800$  Å for the hot electrons at 4.2 K. This is considerably larger than previous reports for devices with heavier doping in the base.<sup>6,7</sup> The interpretation of the energy distributions which are centered around  $V_{\text{peak}} = 0$  for all injection levels should be different for  $V_{CB} > 0$  and  $V_{CB} < 0$ . For the negative range the distribution shape is approximately correct since the barrier height is  $\simeq \Phi_C + |V_{CB}|$ . However, for the positive range  $\Phi'_C = kV_{CB}$ , where  $k$  may depend on  $V_{CB}$ . Thus, the true distribution is estimated by multiplying the measured one by  $1/k$ . This leads to a complete energy distribution associated with the normal momentum to the barrier with a peak below the AlGaAs barrier top. Note that  $\alpha$  is 0.15 at  $V_{CB} = 0$  V with  $\Phi'_C \simeq 210$  meV and 0.7 at  $V_{CB} = 0.9$  V with  $\Phi'_C$  estimated to be about 100 meV (this is the approximate value of  $\Delta E_C$  at the interface where  $x = 0.12$ ). Thus, 85% of the carriers have "normal" energy less than 210 meV and 30% of them have normal energy less than  $\sim 100$  meV above the bottom of the conduction band at the collector boundary. From this we can estimate that the normal energy peak must be somewhat below halfway between 100 and 210 meV above the bottom of the conduction band. Note that the Fermi level is about 18 meV above the conduction band in the base, and the accumulation at the base-collector interface bends the conduction band by some 60 meV more. Thus, the distribution peak is somewhat in the range 40–70 meV above the Fermi level in the base, and upon biasing only the high-energy tail of the distribution is collected. Moreover, since  $\alpha$  and the

energy distributions do not change with injected electron energy, it seems that the electrons always thermalize to the same level and much more quickly than would be expected from a phonon emission mechanism.<sup>12</sup> The final low-energy levels, which they reach the collector with, implies that they are  $\Gamma$  electrons, even though  $eV_{BE}$  is above the bottom of both  $L$  and  $X$  valleys (which are 0.36 and 0.51 eV above the bottom of the  $\Gamma$  band minimum, respectively).

To conclude, we have reported the fabrication and characterization of a heterojunction THETA device. While at room temperature thermionic emission dominated, at temperatures below 160 K tunneling was dominant. Hot electrons had an effective mean free path of 2800 Å in a  $2 \times 10^{17}$  cm<sup>-3</sup>  $n$ -type GaAs base. The transfer ratio in a device with an 1100-Å base width was 0.7 at 4.2 K, with a weak temperature dependence. Energy distributions of the hot electrons at the collector were estimated to be some  $\sim 150$  meV above the Fermi energy, with a peak distribution only slightly above the Fermi energy. Thus, electrons lost most of their initial energy as they traversed through the base. The exact mechanism of transfer through the base is not clear, but this type of device is useful for studying hot-electron effects, in addition to its inherent potential as a very fast device.

We would like to acknowledge W. P. Dumke for helpful discussions, P. M. Solomon and F. Stern for carefully reading the manuscript and giving their suggestions, J. W. Mitchell for the ion implantation, and L. Osterling for his technical assistance. This work was supported by NRL grant No. N00014-82-C-2369.

<sup>1</sup>C. A. Mead, Proc. IRE **48**, 359 (1960); J. Appl. Phys. **32**, 646 (1961).

<sup>2</sup>M. Heiblum, Solid State Electron. **24**, 343 (1981).

<sup>3</sup>J. M. Shannon, IEE J. Solid State Electron Devices **3**, 142 (1979); J. M. Shannon and A. Gill, Electron. Lett. **17**, 621 (1981).

<sup>4</sup>R. J. Malik, M. A. Hollis, L. F. Eastman, D. J. Woodard, C. E. C. Wood, and T. R. AuCoin, Proceedings of Conference on Active Microwave Devices (Cornell University, Ithaca, NY, 1981), p. 87.

<sup>5</sup>M. A. Hollis, S. C. Palmateer, L. F. Eastman, N. V. Dandekar, and P. M. Smith, Electron Device Lett. **EDL-4**, 440 (1983).

<sup>6</sup>J. R. Hayes, A. F. J. Levi, and W. Wiegmann, Electron. Lett. **20**, 851 (1984); Phys. Rev. Lett. **54**, 1570 (1985).

<sup>7</sup>N. Yokoyama, K. Imamura, T. Ohshima, H. Nishi, S. Muto, K. Kondo, and S. Hiyamizu, Technical Digest of IEDM (IEDM, San Francisco, CA, 1984), p. 532.

<sup>8</sup>M. Heiblum, E. Mendez, and L. Osterling, J. Appl. Phys. **54**, 6982 (1983).

<sup>9</sup>R. C. Miller, D. A. Kleinman, and A. C. Gossard, Phys. Rev. B **29**, 7085 (1984).

<sup>10</sup>T. Hickmott, P. M. Solomon, R. Fischer, and H. Morkoç, J. Appl. Phys. **57**, 2844 (1985).

<sup>11</sup>M. Heiblum, M. Nathan, and M. Eizenberg, Appl. Phys. Lett. **47**, 503 (1985).

<sup>12</sup>W. P. Dumke (unpublished).